Isothermal Curing of an Uncatalyzed Dicyanate Ester Monomer: Kinetics and Modeling

OLIVIER GEORJON, JOCELYNE GALY,* and JEAN-PIERRE PASCAULT

Laboratoire des Matériaux Macromoléculaires, URA CNRS No. 507, Institut National des Sciences Appliquées de Lyon, 20, Avenue A. Einstein, 69621 Villeurbanne Cedex, France

SYNOPSIS

The isothermal cure of a dicyanate ester monomer has been studied under different atmospheres (air and argon) without any catalyst, by following the evolutions of both glass transition temperature and conversion. Independently of both atmosphere and temperature of cure, there is a unique one-to-one relationship between these two parameters, correctly described by a restated DiBenedetto's equation. The chemical kinetics are satisfactorily modeled with two competing reactions schemes, which are second-order and second-order autocatalyzed, the latter displaying more relative importance under air-curing conditions. Whatever the cure temperature may be, gelation occurs around 0.60 conversion under air, whereas the theoretical $x_{gel} = 0.50$ is experimentally observed under argon. The time–temperature–transformation diagrams have been established. © 1993 John Wiley & Sons, Inc.

INTRODUCTION

Cyanate esters are among the most attractive new thermostable polymers to which a lot of interest has been devoted over the past few years. Thanks to their high fracture toughness and high service temperatures, they meet most of the severe composite applications requirements.[1,2] In addition, the evolution of the electronics industry toward increased circuit densities and operating temperatures exhibited the limits of epoxy-based resins. On the other hand, polycyanurate systems offer very low dielectric losses, which is essential to meet the more stringent insulation resistance requirements.[3]

In the 1980s, Hi-Tek Polymers manufactured a series of aromatic dicyanate commercial products, based on bisphenol derivatives containing the —O—C≡N functional group.[4] Upon heating, they undergo polycyclotrimerization[5,6] that can be catalyzed by transition metal cations and an active hydrogen initiator.[7,8]

This work deals only with the curing kinetics of the uncatalyzed bisphenol A dicyanate, which ap-

peared to us as a model system for the study of a thermosetting material undergoing gelation and vitrification. An inert curing atmosphere (helium, argon, nitrogen . . .) is required to ensure a rigorous experimental procedure. On the other hand, one should keep in mind that such care is not achieved in industrial conditions, where both prepregs manufacturing and final molding are performed without any precautions as for the atmosphere. Hence, it is of real interest to carry out the study under both argon and air (with oxygen and residual moisture) to investigate the influence of the curing atmosphere on the kinetics of the cyanate polymerization. Differential scanning calorimetry is a convenient way to perform such an investigation since it allows monitoring of the reaction throughout the entire range of cure.

The final aim of this work was to be able to prepare networks with different conversions and to measure the evolution of the physical and mechanical properties vs. conversion between the gel point (x_{gel}) and the full cure, as it has been done previously for epoxy–diamine systems.[9] Other experiments are in progress in our group on the chemistry of the dicyanate network formation, especially on the influence of moisture sorption.

EXPERIMENTAL

Materials

The dicyanate monomer chosen for this study is 4-4'-dicyanato-2-2' diphenyl propane (Arocy B10, Rhône-Poulenc Inc., Louisville, KY), supplied as a white high purity (> 99.5%) crystalline powder (melting point: 79°C). It was used as received, without any catalyst. Impurities may result from the synthesis of the monomer and can be monocyanate–monophenol, bisphenol, or/and metal complexing ions.[4] The chemical structure of the monomer, of the monofunctional compound (cumyl phenyl cyanate), and the trimerization reaction involved in the polymerization mechanism are reported in Figure 1.

Procedure

Most of the experiments in this study were performed using differential scanning calorimetry (DSC) (Mettler TA3000). A small amount of monomer (15 ± 5 mg) was transferred into a small DSC aluminum pan, sealed with a holed aluminum lid. Sealed samples were cured either in a thermo-controlled oven, under continuous air flow, or directly in the DSC cell, under argon. Isothermal curing was carried out at five different temperatures (T_c = 150, 165, 200, 225, and 250°C). After various curing times, ranging from 5 min to 5 days, each sample was quenched to room temperature.

All samples were then subjected to a DSC temperature scan from −100 to 400°C at 10°C/min to determine both the glass transition temperature, T_g, of the partially cured material, and the residual heat of reaction, ΔH_R. One must emphasize that all samples, even those cured under air, were scanned under argon, since rigorous measurements require inert conditions to avoid any disturbances by the experimental atmosphere.

Samples that had vitrified during the curing process ($T_g \geq T_c$) could undergo physical aging. Those exhibited an endothermic relaxation peak in the glass transition region, preventing an accurate measurement of T_g. These specimens were first heated
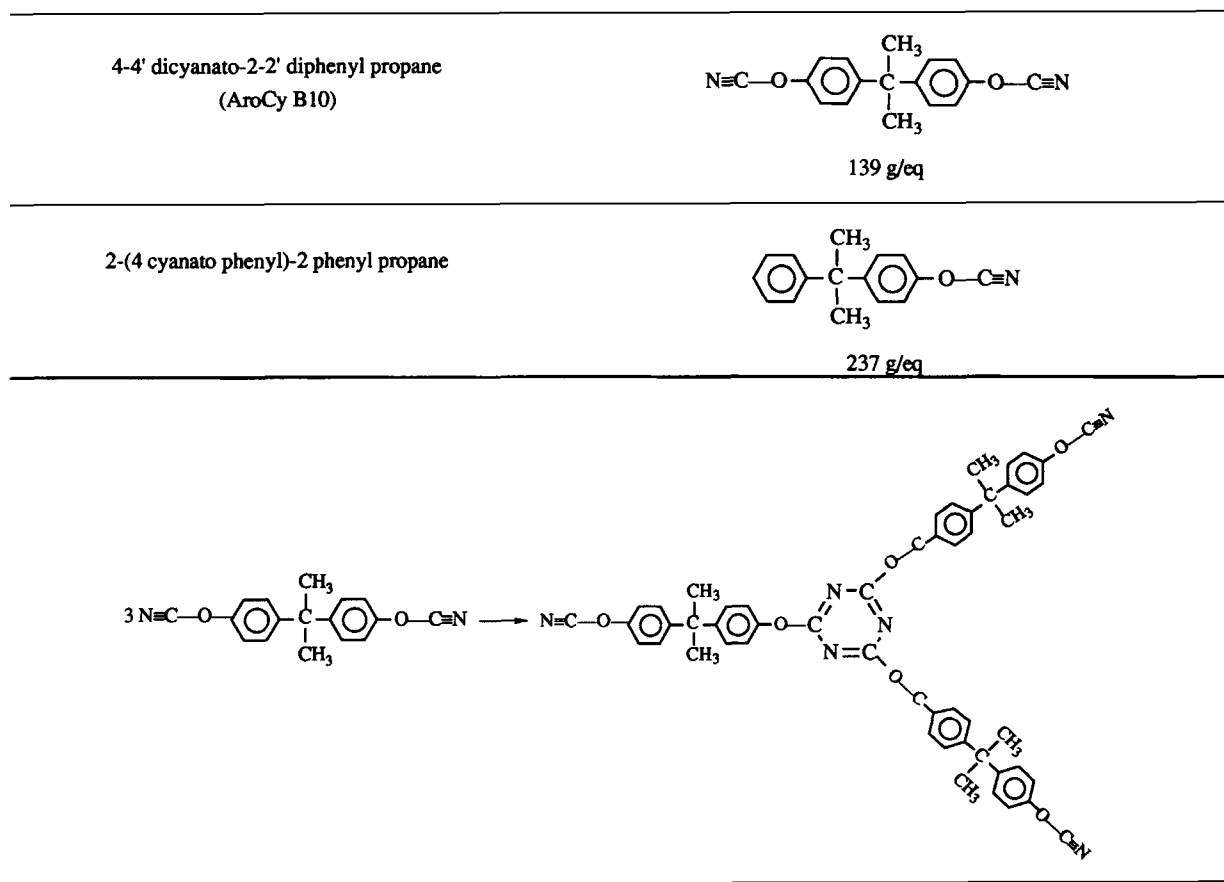

Figure 1   Molecular structure of reactants and trimerization reaction of dicyanates.

up to the peak temperature, quickly quenched, and rescanned to 400°C.

Two typical DSC scans are shown in Figure 2. In the first one [Fig. 2(a)], which corresponds to an early stage of polymerization, T_g appears as an endothermic shift of isobaric heat capacity. In this case, T_g was taken as the onset of the transition. The second one [Fig. 2(b)], which corresponds to the latest stages of reaction, does not display the usual step. In such a case, T_g reaches the temperature range where polymerization is likely to occur. Thus, as early as the relaxation begins, the reaction starts and the endothermic shift is hidden by the exothermic peak. For such an experiment, T_g is taken as the onset of the polymerization peak.

In both cases, the residual heat of reaction of the remaining reactants appears as an exothermic peak. ΔH_R is deduced as usual by integrating the area between the heat flow curve and the base line. With the rate we use throughout all this study (10°C/ min), we admit that the heating provided under argon is quick enough to prevent any thermal degradation phenomenon (see later). Then, assuming a single reaction mechanism, the extent of reaction can be calculated by[10]

$$x = \frac{\Delta H_T - \Delta H_R}{\Delta H_T} \tag{1}$$

where ΔH_T (the total heat of reaction) is determined in the same way by integrating the reaction peak of an initially unreacted specimen from 220 to 350°C. It was found to be 710 ± 15 J/g.

Some workers[11,12] prefer to use eq. (2) rather than eq. (1) to calculate conversion:

$$x = \frac{\Delta H_T - \Delta H_R}{\Delta H_0} \tag{2}$$

These workers suggest that full conversion cannot be achieved because of steric hindrance in the latest stages of reaction. Hence, a distinction must be made between ΔH_T and ΔH_0, which is the true enthalpy of reaction, determined with model compounds or by titration methods.

We carried out a few experiments with the highly volatile monofunctional compound, for which steric hindrance cannot occur. To prevent any weight loss, we used in this case sealed stainless steel large-volume medium-pressure pans. Since we found no significant differences between the reaction enthalpies of both compounds (expressed in joules by the cyanate equivalent), we considered eq. (1) as a correct way to compute conversion.
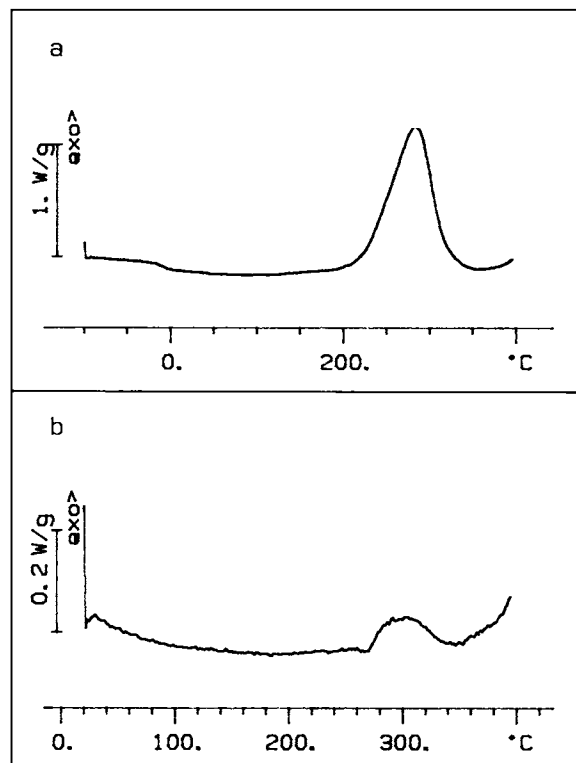

Figure 2 DSC scans of partially reacted samples: (a) early stages of cure; (b) latest stages of cure.

We also performed Fourier transformed infrared spectroscopy (FTIR) to check the validity of conversions determined with DSC in the latest stages of reaction. This analysis was carried out on a Nicolet MX-1 spectrometer, with KBr pellets containing the finely ground material. As advised by the supplier,[13] the C — H stretch band (2875 cm^{-1}) was used as an internal standard, since it is assumed to be unmodified during trimerization. Infrared absorption of nitriles (— C≡N stretching vibration) appears as a double band (2270–2240 cm^{-1}). Conversions were calculated using the height of the 2270 cm^{-1} band with respect to the height of the reference band.

In addition, the gel time was detected for each cure temperature under both curing atmospheres by the appearance of insoluble particles in a solution obtained with 1% of partially cured material dissolved in a polar solvent such as tetrahydrofurane (THF).

RESULTS AND DISCUSSION

Relationship between T_g and x

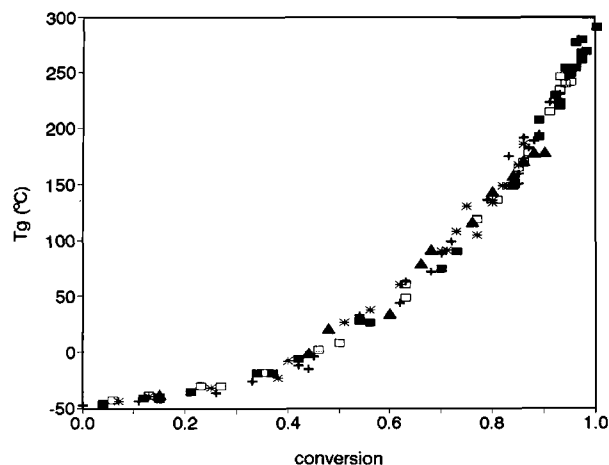Figures 3 and 4 display the glass transition temperatures plotted as a function of the extent of cure. In

Figure 3 Glass transition as a function of conversion: (■) $T_c = 250°C$; (□) $T_c = 225°C$; (+) $T_c = 200°C$; (✻) $T_c = 165°C$; (▲) $T_c = 150°C$.

Figure 3, the different symbols correspond to different curing temperatures, whatever the curing atmosphere may be, whereas they depend only on the atmosphere (air or argon) in Figure 4, independently of the temperature of cure.

It is obvious for this system that there is a unique one-to-one relationship between T_g and x. Neither the curing atmosphere nor the curing temperature has a significant influence on the glass transition temperature reached by the material at a given conversion. This was expected since one assumes that there is only one product formed by the curing reaction of our dicyanate ester system. Nevertheless, the curing atmosphere or/and the temperature could have a slight influence on the network structure, without modifying significantly T_g. As a consequence, the glass transition temperature can be used in our case to measure the conversion.

We may remark that the glass transition temperature of the commercial product B30 (the 30% trimerized resin of bisphenol A dicyanate, supplied by Rhône-Poulenc Inc.) matches correctly our data at 0.3 conversion ($-21°C$).

Moreover, the absence of discontinuity throughout the entire range of cure supports the consistency of our two different ways of measuring T_g. Increase of T_g when x approaches 100% is very sharp. Thus, T_g is a more sensitive parameter than is x to describe the final stages of reaction.

A considerable amount of work has been done to find either empirical or theoretical equations to describe the relationship between T_g and x for various thermosetting polymers.[11,12,14,15] Among them, DiBenedetto's equation, as reported by Nielsen,[16] is

one of the easiest approaches to adjusting the experimental T_g vs. x.

The glass transition temperature of a (partially) cured thermoset up to an extent of reaction x is given by

$$T_g = T_{g0} + \frac{(T_{g\infty} - T_{g0})\lambda x}{1 - (1 - \lambda)x} \qquad (3)$$

where T_{g0} and $T_{g\infty}$ are, respectively, the glass transition temperatures of the monomer and of the fully reacted network.

From an extension of Couchman's approach,[17] Pascault and Williams[15] showed that λ (which is originally taken as an adjustable parameter) is, in fact, the ratio $\Delta C_{p\infty}/\Delta C_{p0}$, where ΔC_{p0} and $\Delta C_{p\infty}$ are the isobaric heat capacity changes in the glass transition region of the monomer and of the fully reacted network, respectively. DiBenedetto's equation, as developed by Pascault and Williams, is a true theoretical description of T_g vs. x, in which all parameters are easily measurable by the DSC technique.

Table I reports the value of $T_{g\infty}$, T_{g0}, $\Delta C_{p\infty}$, and ΔC_{p0} for our system. These are the means of eight measurements. Crystalline samples were melted and quickly quenched to $-100°C$ to determine T_{g0} and ΔC_{p0}. It should be pointed that $T_{g\infty}$ and $\Delta C_{p\infty}$ were evaluated in two different ways:

- by rescanning monomer samples first heated up to the end of the exothermic reaction peak in a first scan; and
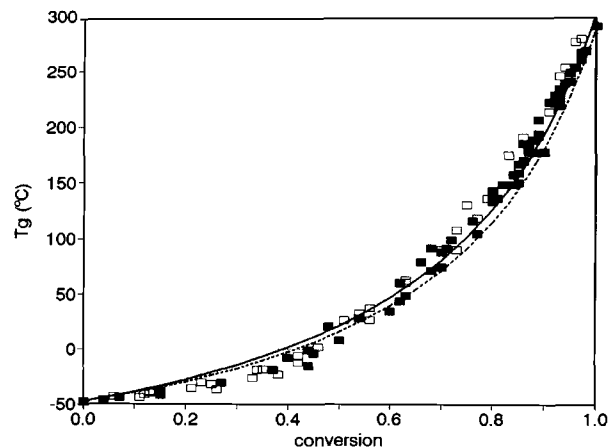- by scanning a sample first cured in the oven for 5–7 h at 250°C.

Figure 4 Glass transition as a function of conversion: (■) cure under air; (□) cure under argon; (- - - - -) DiBenedetto equation; (——) restated DiBenedetto equation.

Table I Characteristic Temperatures and Isobaric Heat Capacity Changes in the Vicinity of the Glass Transition for the Dicyanate Monomer and the Final Network

Polymer	$t = 0$	$t = \infty$
T (°C)	$T_{m_0} = 79 \pm 1$ $T_{g_0} = -48 \pm 1$	$T_{g_\infty} = 292 \pm 2$
ΔC_p (J/g/K)	$\Delta C_{p_0} = 0.56 \pm 0.06$	$\Delta C_{p_\infty} = 0.13 \pm 0.02$

The value of λ obtained (0.23) is lower than that measured by Jordan et al. (0.32)[9] for an epoxy–diamine system or those reported by Pascault and Williams[15] for several epoxies networks ($\approx$ 0.5). This difference is due mainly to a difference in ΔC_{p_∞} (much lower value for the cyanate system) rather than in ΔC_{p_0}. Hence, among the matrices cited, our network displays the less segmental mobility, thus the sharpest increase of T_g in the latest stages or cure.

The dashed line in Figure 4 is the plot of eq. 3 computed with the parameters values listed in Table I. There is a rather good agreement with experimental measurements, but all the latter are above DiBenedetto's curve for x greater than 0.6.

The assumption we made that T_{g_∞} corresponds to an extent of cure equal to 100% is then open to serious question. Indeed, topological limitations at the end of cure might prevent unreacted cyanate groups spatially separated from each other to react, due to the high connectivity of the final network, the same as for epoxy systems.[9]

To take this into account, a restated equation can be used[12]:

$$T_g = T_{g_0} + \frac{(T_{g_M} - T_{g_0})\lambda' x'}{1 - (1 - \lambda')x'} \qquad (4)$$

with $x' = x/x_M$ and $\lambda' = (\Delta C_{p_M})/(\Delta C_{p_0})$. x_M is the perfectly known extent of reaction of an almost fully cured network showing $T_g = T_{g_M}$ and $\Delta C_p = \Delta C_{p_M}$. In other words, it means that the polymer at any conversion can be modeled as a random mixture of an x_M polymer and monomer, instead of a mixture of a fully reacted network and monomer as in eq. (3).

We applied eq. (4) to our system with $x_M = 0.95$ and $T_{g_M} = 243$°C. A serious problem lay in the determination of ΔC_{p_M}, since, in that case, the endothermic shift in the thermogram is hidden by the exothermic reaction peak [see previous section and Fig. 2(b)]. We were compelled to use ΔC_{p_M} as an adjustable parameter for the T_g–x relationship, determined from the plot of $(T_{g_M} - T_{g_0})/(T_g - T_{g_0})$

vs. $1/x'$ (not shown here). The value obtained is $\Delta C_{p_M} = 0.16$, which seems to be reasonable since it is a little more than $\Delta C_{p_\infty} = 0.13$ and lower than $\Delta C_p = 0.18$ for $x = 0.85$, the last value that we can measure.

The plot of eq. (4) is shown on Figure 4 (solid line). The adjustment is excellent all over the conversion range, especially at high conversions. Putting $x = 1$ in eq. (4) leads to a new "virtual" value for T_{g_∞} of 305°C. The maximum observed T_g (292°C) corresponds with a degree of cure x_{max} equal to 0.99, which must be considered as a maximum reachable conversion value. We may notice that such a difference between x_{max} and 100% conversion lies in the measurement uncertainty of the DSC technique.

This result is supported by the FTIR analysis. Indeed, this technique allows detection of the presence of all the unreacted cyanate groups, whereas DSC detects only the functions liable to react. Thus, the conversion x_{IR} calculated by the FTIR technique is the true conversion x, obtained without any assumption. On the other hand, the quantities ΔH_T and ΔH_R measured by DSC are proportional to x_{max} and $(x_{max} - x)$, respectively. Hence, x_{DSC} [see eq. (1)] is equal to x/x_{max}, which yields that, for given curing conditions, the ratio x_{IR}/x_{DSC} is a measure of x_{max}. Results after 24 h at 225°C are the following: $x_{DSC} = 0.99$ and $x_{IR} = 0.98$. Therefore, we get again $x_{max} = 0.99$. It should be noted that other works available in the literature[13,18–20] report favorable comparison between conversions measured by both DSC and FTIR techniques.

Thus, although we cannot deny the effect of steric hindrance in the very latest stages of cure, x_{max} is very close to 1, which explains why we found no significant differences between the reaction enthalpies of mono- and dicyanate. We can therefore consider DSC as an adequate technique to determine easily the conversion of our system, either by integrating the reaction peak and using eq. (1) or by measuring T_g and using eq. (4) to compute x.

Gel Point

The gel times, times for which one observes the appearance of insoluble particles, and the corresponding degrees of cure x_{gel} determined by DSC are reported in Table II, for each cure temperature T_c and for each cure atmosphere. In opposition to the previous section, where the atmosphere had no measurable influence on the T_g reached by the material at a given conversion, one notices that the conversions at gelation are significantly different depending on whether the curing occurs under air or argon. On the other hand, x_{gel} is almost constant, irrespective of the curing temperature T_c, within the measurement uncertainty. It ranges from 0.58 to 0.67 under air and from 0.50 to 0.53 under argon, both times in regions where the extent of reaction raises quickly, preventing a more accurate determination. The corresponding glass transition temperatures, $_{gel}T_g$, are nearly 50°C under air and 30°C under argon. In both cases, it is below the melt temperature of the crystalline monomer. Thus, $_{gel}T_g$ is not attainable with isothermal cures.

There was a conflict in the literature concerning the gel conversion of homopolymerized cyanate esters. The value predicted by the mean-field theory (0.5) had been experimentally observed only by Bauer and Bauer,[21] using DSC and IR and extrapolating plots of gel fraction w_g vs. conversion, whereas Gupta and Macosko[22] and Osei-Owuzu et al.[8,23] reported values ranging from 0.60 to 0.65, measured by DSC, NMR, and IR. For their own part, Simon and Gillham[20,24] found 0.64 with bisphenol M dicyanate, using dynamic mechanical methods. Gupta and Macosko[22] proposed the cyanate trimerization to be diffusion-controlled rather than kinetically controlled. Other authors[25] tried to develop models taking into account substitution effects (i.e., different reactivities of cyanate groups depending on whether the monomer is unreacted or is already linked to a forming cluster), which could

Table II Gel Times and Corresponding Extents of Cures as a Function of the Cure Temperature

| T_{cure} (°C) | Gel Time | | x_{DSC}^{gel} | |
	Air	Argon	Air	Argon
250	24 min	23 min	0.67	0.50
225	50 min	54 min	0.63	0.53
200	120 min	140 min	0.58	0.50
165	9 h	8 h	0.65	0.51
150	27 h	—	0.67	—

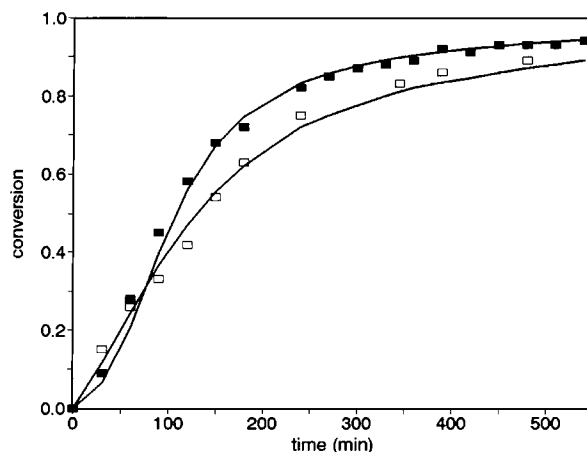**Figure 5** Conversion as a function of time (T_c = 200°C): (■) under air; (□) under argon; (——) model calculations.

explain a shift toward higher values of x_{gel}. Nevertheless, this explanation is not really appealing, since the two cyanate groups on a same monomer seem to be sufficiently separated from each other to prevent any substitution effect.

What we find under inert conditions matches the theoretical value, whereas our results with curing under air meet with the values cited above (0.60–0.65). This large difference between the two values makes us fully aware of the main importance of the curing atmosphere on the polymerization of cyanate esters. Indeed, Bauer and Bauer[21] used inert conditions, while Macosko and Gupta[22] and Osei-Owuzu et al.[8,23] performed their studies under air. Simon and Gillham[20,24] carried out curings under helium, but detected gelation through an indirect way (dynamic mechanical measurements, with an impregnated glass braid with possible moisture on its surface). Before the present study, the only one performed under argon with direct detection of the gel point (a plot of gel fraction w_g vs. x)[21] reported gel conversions that correctly matched the theoretical value. It is likely that curing cyanates under air leads to side reactions between residual water and cyanate groups that contribute to the disappearance of cyanate units (i.e., increase of conversion) without forming triazine ring branching points, hence, delaying gelation in terms of conversion. Even with that, the mechanism leading to a higher value of x_{gel} under air is still not well understood.

Evolution of Conversion with Time

Figure 5 shows the variation of the extent of reaction vs. time for the isothermal cures (under air and argon) at 200°C. Similar curves are obtained at the

other temperatures. Lines represent the calculated variation of x with time issued from the model that will be discussed in the next section.

Again, one can see that different atmospheres result in significantly different behavior of cyanates during their curing. The curve $x = f(t)$ obtained under air displays a more pronounced sigmoidal shape than does the one obtained under argon. Such an S-shape indicates an autocatalytic character of the reaction involved. To elucidate this phenomenon, it is essential to find an appropriate equation to model the kinetics of our system, either under air or argon.

Kinetics Modeling of Dicyanate Homopolymerization

Several workers[25-29] tried to model the kinetics of the cyanate trimerization. Gupta[29] and Williams et al.[25] proposed a model to predict the relative concentration of clusters of different sizes (trimer, pentamer, heptamer, . . .) as a function of the conversion. Gupta[29] assumed equal reactivity of all functional units, whereas Williams[25] took into account possible substitution effects. Works are in progress in our group[26] to correlate the theoretical with experimental results. Our proposal here, more simple, is to try to have a general equation $(dx)/(dt) = f(x, T)$ to describe the overall kinetic scheme.

Recently, we became aware of an interesting work by Simon and Gillham[19,20,24] in this area. The authors were inspired by previous work from Bauer et al.[27] who observed the reaction to be second-order autocatalytic. They proposed a mechanism involving the formation of an intermediate imidocarbonate by reaction of cyanate groups with impurity phenolic OH groups resulting from the synthesis of the monomer (monocyanate–monophenol or diphenol):

$$Ar\!-\!OH + Ar\!-\!OCN \;\rightarrow\; Ar\!-\!O\!-\!\underset{\underset{NH}{\|}}{C}\!-\!OAr \quad (5)$$
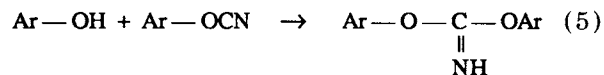
This imidocarbonate can react with two OCN groups to form the stable triazine ring and regenerate the phenolic group, which can enter into reaction (5) again:

$$Ar\!-\!O\!-\!\underset{\underset{NH}{\|}}{C}\!-\!O\!-\!Ar \;+\; 2ArOCN \;\longrightarrow\; \text{(triazine ring)} \;+\; ArOH \quad (6)$$
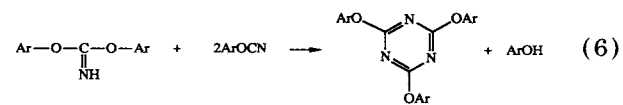
In fact, the reaction does not occur if absolutely pure dicyanate is heated without a catalyst. The starting reaction is caused by an impurity (ArOH/metal ions)-catalyzed scheme besides the autocatalytic one. In that case, the intermediate imidocarbonate is stabilized by the metal complex.

Simon and Gillham modified the model of Bauer et al. by assuming that the reaction of cyanate ester with aryl phenol [eq. (6)] is an equilibrium reaction, as has been observed by Shimp et al.[30] It yields the following rate reaction:

$$\frac{dx}{dt} = k_1(1 - x)^2 + k_2 x(1 - x)^2 \quad (7)$$

where k_1 and k_2 are the rate constants for the second-order and second-order autocatalyzed reaction, respectively. It should be pointed that k_1 and k_2 incorporate the effect of temperature and the concentration of aryl phenol impurity and that k_1 may include eventually the concentration of metal complexing ions, as catalysts or impurities. All the impurity concentrations are assumed to be unchanging if only one batch of monomer is used, which is the case in the present study.

It should be pointed out that this model cannot account for the different kinetics that we observe under air and argon, since the impurity concentrations are the same in both cases. But one must keep in mind that the chemical species presumably responsible for the different behavior under air and argon is water, which can react with cyanate in a similar way as aryl phenol, forming an intermediate (eq. (8)) that can be stabilized by carbamate formation or by triazone formation,[20] regenerating water which can enter into reaction (8) again.

$$H_2O + Ar\!-\!OCN \;\rightarrow\; Ar\!-\!O\!-\!\underset{\underset{NH}{\|}}{C}\!-\!OH \quad (8)$$
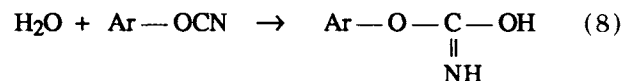
As a consequence, it is possible to include the reaction of cyanate with adventitious water by simply assuming that the constants k_1 and k_2 of the model incorporate both aryl phenol impurities and residual water concentrations.

We used a Runge–Kutta algorithm to compute, for each cure temperature, the values of k_1 and k_2 that best fitted our data. As eq. (7) is valid only if the reaction is kinetically controlled, we rejected x values for which the corresponding T_g is above the cure temperature, since we cannot exclude a priori the possibility of a diffusion-controlled reaction after vitrification. The best $(k_1; k_2)$ were determined by minimizing the least-square difference between ex-

Table III   Activation Energies and Pre-Arrhenius Frequency Factors for the Rate Constants of the Model

Atmosphere	A_1 (min^{-1})	A_2 (min^{-1})	E_{a_1} (kJ/mol)	E_{a_2} (kJ/mol)
Air	4.96	3.0×10^8	34.9	87.7
Argon	92.9	1.1×10^8	41.8	89.0

perimental and calculated values, considering independently the $(x; t)$ data under air and argon at each curing temperature T_c.

Lines in Figure 5 represent the calculated curves $x = f(t)$ at 200°C, under argon and under air. Agreements with the experimental data are excellent all over the conversion range. Hence, the autocatalytic model seems to describe correctly the kinetics of our system.

k_1 and k_2 are expected to depend on temperature with the Arrhenius laws:

$$k_i = A_i \exp\left(\frac{-Ea_i}{RT}\right) \quad i = 1 \text{ or } 2 \qquad (9)$$

Arrhenius plots ($\ln k = f(1/T_c)$) for k_1 and k_2 display good linearity, although the correlations for k_1 values (0.91 and 0.86) are rather poor compared with those obtained for k_2 (0.99). This may be attributed to the fact that the impurity-catalyzed reaction path is significant only in the very early stages of reaction. Thus, k_1 is computed only with the two or three first experimental data, which may lead to imprecise calculated values. This can explain also why the adjustment between calculated and experimental conversions is slightly less accurate in the early stages of reaction (see Fig. 5).

The different values for activation energies and pre-Arrhenius frequency factors determined with the data under both atmospheres are compared in Table III. First of all, one can notice the remarkable consistence between the activation energies, which are nearly the same (within the determination uncertainty) under both atmospheres. This was a *sine qua non* condition for the validity of the model, since the phenomena invoked are similar in both cases. The relative temperature dependence of the two rate constants appears to be consistent also with the mechanism assumed, as already pointed out by Simon and Gillham.[19] As a matter of fact, it is normal to find Ea_1 lower than Ea_2, since metal complexing ion impurities are expected to be intrinsically more efficient catalysts than are the species involved in the autocatalytic path.

Concerning the frequency factors, it is obvious with both curing conditions that A_2 is several orders of magnitude greater than A_1. These relative values were expected since k_1 is assumed to include the concentration of metal impurities, which is announced by the supplier to be less than 100 ppm. k_2 is three times greater under air than under argon, because in the former case, the autocatalytic scheme is more important due to the presence of the adventitious moisture in air. An other series of results supports this conclusion: Figure 6 reports the maximum exotherm temperature of the residual reaction heat during a DSC scan, T_{max}, plotted as a function of conversion[26] for both types of curing, under air and argon. T_{max} goes through a minimum as conversion increases. This behavior, typical of an autocatalytic scheme (a partially cured sample is more reactive than is an unreacted one) is more pronounced with the data obtained after cure under air than those corresponding to cures under inert atmosphere. The difference in k_1 values (greater under argon than under air) is hardly explainable, except if one invokes the very small values of k_1 compared with k_2: It is difficult to evaluate accurately the cat-
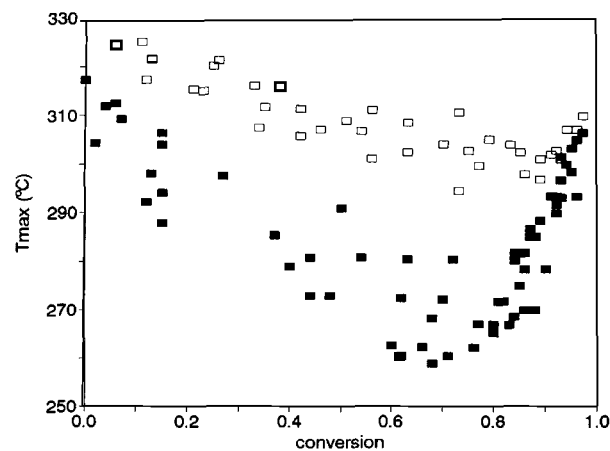

Figure 6 Exotherm maximum temperature during a DSC scan as a function of conversion: (■) after cure under air; (□) after cure under argon.

alytic phenomenon because it is largely covered by the autocatalytic one.

It should be noted that the large differences in Ea_i and A_i indicate that our assumption of a single reaction mechanism for conversion measurements by DSC is not truly correct, but one must keep in mind that the catalyzed scheme occurs only when the reaction begins or/and if the cure is performed at a low temperature. For most of the DSC runs, the extents of cure reached by the specimens during the isothermal cure are enough for the catalyzed reaction path to be insignificant. Anyway, the residual polymerization takes place at high temperatures ($> 200°C$) for which $k_1 \ll k_2$.

Test of the Kinetics Model: Evolution of T_g with Time

A test of the proposed kinetics has been accomplished comparing experimental and calculated glass transition temperatures.

Integration of eq. (7) leads to

$$t = \frac{1}{k_1 + k_2}\left(\frac{k_2}{k_1 + k_2} \ln\left(\frac{k_2/k_1\, x + 1}{1 - x}\right) + \frac{x}{1 - x}\right)$$

(10)

Thus, we can, for each curing atmosphere,

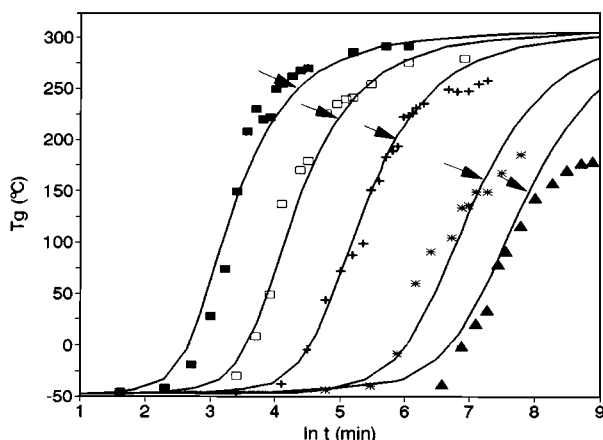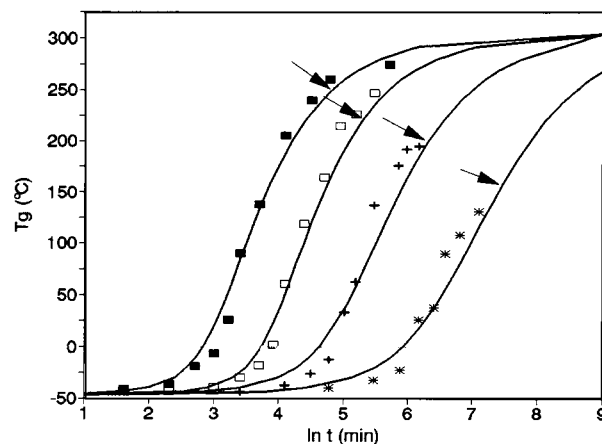(i) determine with eq. (4) the extent of reaction corresponding with each T_g between T_{g_0} and T_{g_∞};

Figure 7 Glass transition temperature as a function of ln(cure time) (cure under air): (■) $T_c = 250°C$; (□) $T_c = 225°C$; (+) $T_c = 200°C$; (✳) $T_c = 165°C$; (▲) $T_c = 150°C$; (——) model calculations. Vitrification onsets are marked by arrows.

Figure 8 Glass transition temperature as a function of ln(cure time) (cure under argon): (■) $T_c = 250°C$; (□) $T_c = 225°C$; (+) $T_c = 200°C$; (✳) $T_c = 165°C$; (——) model calculations. Vitrification onsets are marked by arrows.

(ii) calculate k_1 and k_2 for each cure temperature T_c, assuming the validity of the Arrhenius laws and the constants A_1, A_2, Ea_1, and Ea_2 mentioned above; and

(iii) compute with eq. (10) the time to reach a specified T_g at a specified cure temperature.

Figures 7 and 8 show the plots of experimental T_g and the curves calculated with this procedure against the logarithm of curing time for the five isothermal curing temperatures, under air and argon, respectively. We must remember at this point that there are three possible causes of imprecise calculated values, i.e., the two Arrhenius regressions for k_1 and k_2, with rather poor correlations for the former, and the DiBenedetto's modified equation used to convert T_g into x. Nevertheless, the agreement between experiments and the model is satisfactory for each cure temperature up to the vitrification onsets (marked by arrows), after which the experimental points branch off from the calculated curves. One can invoke there a change from chemical-controlled to diffusion-controlled kinetics in the vicinity of isothermal vitrification. This results in a lowered reaction rate, especially at low temperatures. The composite reaction mechanism used in this study does not lead to parallel $T_g = f(\ln t)$ calculated curves since two different paths with different activation energies are involved. Thus, it is impossible to obtain a single master curve by shifting the T_g data along the ($\ln t$) axis, as can be done with epoxy amine systems, for instance.[10]
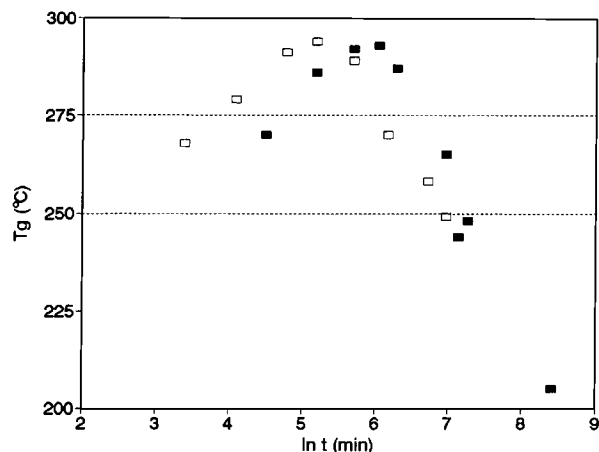
Figure 9 Glass transition temperature as a function of ln(cure time) (cure under air): (■) T_c = 250°C; (□) T_c = 275°C.

Thermal Degradation

We became aware of a surprising phenomenon when we investigated the latest stages of curing under air. Indeed, we observed a decrease of T_g for longer times of cure at 250°C. It may be attributed to thermooxidative degradation in the oven.[31] More experiments at 275°C confirmed such behavior. Figure 9 displays the evolution of glass transition temperature with ln (cure time) for these two cure temperatures, using an expanded scale for the temperature axis. The maximum value is observed earlier at 275°C, as expected, but it is not significantly different from the

one observed at 250°C. Thus, it is impossible to reach 100% conversion with our particular system, because of two phenomena involved in the latest stages of cure:

- steric hindrance
- competition between curing and thermal degradation, especially if the curing is performed under air. Under argon, such a drop of T_g is much less pronounced, though appreciable.

CONCLUSION

Most of the results can be conveniently summarized in the isothermal time–temperature–transformation diagram of B10 without a catalyst shown in Figure 10. For an easier understanding of the figure, we reported only the data obtained with a cure under air.

1. The diagram displays the experimental gelation points, for which the extent of reaction was found to be nearly constant, independent of temperature. The average value (0.65) obtained under air agrees with most results reported in the literature, but is quite different from the one found under argon, which matches the mean-field theory prediction (0.50). We show in this study that the anomalous high conversion at gelation for cyanate systems is most probably due to residual water contained in the curing atmosphere, which
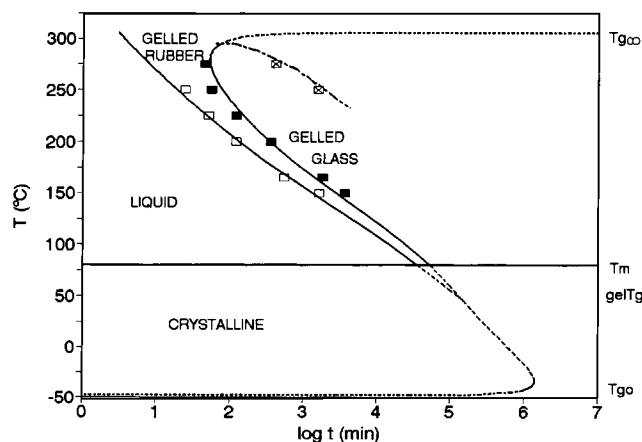

Figure 10 Time–temperature–transformation diagram of uncatalyzed bisphenol A dicyanate under air: (□) gel points; (■) vitrification onsets; (⊠) devitrification points; (———) gelation and vitrification contours issued from model calculations between T_m and $T_{g\infty}$; (----) gelation and vitrification contours issued from model calculations below T_m and above $T_{g\infty}$; (— — —) hand-fitted devitrification contour.

can react with cyanate groups, delaying the appearance of the gel.

2. We reported also experimental vitrification onsets, i.e., the times at which T_g reaches the different cure temperatures. The reaction rate is then slowed down due to a change from chemical-controlled to diffusion-controlled kinetics.

3. The one-to-one correspondence between T_g and conversion, independent of both the cure temperature and of the curing atmosphere, is correctly described by a DiBenedetto's equation as developed by Pascault and Williams. It enables us to convert, when desired, x values given by the model into T_g values. A model that takes into account two competing reactions (which are second-order and second-order autocatalyzed, respectively) describes satisfactorily the trimerization reaction as far as it is kinetically controlled, i.e., up to the vitrification onset. The autocatalytic path has more relative importance under air than under argon, because of the moisture involved in the reaction. Using this model, gelation (x = 0.60) and vitrification (T_g = T_c) curves can be calculated. They are plotted (solid lines) in Figure 10 and provide excellent fitting with experimental data.

4. Calculated gelation and vitrification curves are plotted using dashed lines if they correspond to values that cannot be attained by isothermal curing conditions, i.e.:

• below 79°C, which is the melt point of the naturally crystalline monomer;

• above 292°C, which is the maximum observed value for T_g, since both steric hindrance and thermooxidative degradation under air prevent the network to undergo a complete cure up to 100% conversion.

5. An alternate line represents the hand-fitted devitrification curve, related to the thermooxidative behavior of our system. When long cures at high temperatures are performed under air, one observes a drop of T_g, down through the cure temperature, even if it is below $T_{g\infty}$.

This work is the preliminary part of a further investigation in the properties of cyanate networks. The model presented here does not elucidate completely the mechanism of dicyanate homopolymerization, but is a useful tool to monitor its kinetics.

It allowed us to select different curing schedules to prepare cyanate networks at different conversions, in order to study the evolution of both physical and mechanical properties with conversion. Meanwhile, more work is carried out in our group to understand more deeply the mechanism of the cyanate trimerization.

REFERENCES

1. G. W. Bogan, M. E. Lyssy, G. A. Monnerat, and E. P. Woo, *SAMPE J.*, **24**, 45 (1988).
2. F. W. Lee and M. A. Boyle, in *Plastics, Metals, Ceramics*, H. L. Hornfeld, ed., SAMPE Eur., Switzerland, 1990, Chap. 57.
3. P. C. Yang, E. P. Woo, S. A. Laman, J. J. Jakubowski, and D. M. Pickelman in *36th SAMPE Symposium*, 1991, p. 437.
4. D. A. Shimp, J. R. Christenson, and S. J. Ising, Hi-Tek Publication, Louisville, KY, 1989.
5. J. Bauer, M. Bauer, and H. Much, *Acta Polym.*, **37**, 221 (1986).
6. M. Bauer, J. Bauer, and B. Garske, *Acta Polym.*, **37**, 604 (1986).
7. V. V. Korshak, V. A. Pankratov, A. A. Ladovskaya, and S. V. Vinogradova, *J. Polym. Sci. Chem.*, **16**, 1697 (1978).
8. A. Osei-Owuzu and G. C. Martin, *Polym. Eng. Sci.*, **31**, 1604 (1991).
9. C. Jordan, J. Galy, and J. P. Pascault, *J. Appl. Polym. Sci.*, **16**, 859 (1992).
10. G. K. Wisanrakkit and J. K. Gillham, *J. Coatings. Tech.*, **62**, 783 (1990).
11. H. Stütz, K. H. Illers, and J. Mentes, *J. Polym. Sci. Phys.*, **28**, 1483 (1990).
12. A. Hale, C. W. Macosko, and H. E. Bair, *Macromolecules*, **24**, 2610 (1991).
13. D. A. Shimp, S. J. Ising, and J. R. Christenson, in *International SAMPE Symposium and Exhibition Proceedings*, 1989, Vol. 34 (Part 1), p. 222.
14. A. T. DiBenedetto, *J. Polym. Sci. Phys.*, **25**, 1949 (1987).
15. J. P. Pascault and R. J. J. Williams, *J. Polym. Sci. Phys.*, **28**, 85 (1990).
16. L. E. Nielsen, *J. Macromol. Sci. Rev. Macromol. Chem.*, **C3**, 69 (1969).
17. P. R. Couchman, *Macromolecules*, **20**, 1712 (1987).
18. J. M. Barton, D. C. L. Greenfield, I. Hamerton, and J. R. Jones, *Polym. Bull.*, **25**, 475 (1991).

19. S. L. Simon and J. K. Gillham, *ACS Polym. Chem. Prepr.,* **32**(2), 182 (1991).

20. S. L. Simon, PhD Thesis, Princeton University, 1992; also *J. Appl. Polym. Sci.,* to appear.

21. M. Bauer and J. Bauer, *Makromol. Chem. Macromol. Symp.,* **30,** 1 (1989).

22. A. M. Gupta and C. W. Macosko, *Makromol. Chem. Macromol. Symp.,* **45,** 105 (1991).

23. A. Osei-Owuzu, G. C. Martin, and J. T. Gotro, *ACS Polym. Mater. Sci. Eng.,* **66,** 304 (1992).

24. S. L. Simon and J. K. Gillham, *ACS Div. Polym. Mater. Sci. Eng.,* **66,** 454 (1992).

25. R. J. J. Williams, A. Vasquez, and J. P. Pascault, *Polym. Bull.,* **28,** 219 (1992).

26. V. Mirco, Z. Q. Cao, F. Méchin, and J. P. Pascault, *ACS Polym. Div. Polym. Mater. Sci. Eng.,* **66,** 451 (1992).

27. M. Bauer, J. Bauer, and G. Kühn, *Acta Polym.,* **37,** 715 (1986).

28. J. Bauer and M. Bauer, *Acta Polym.,* **38,** 16 (1987).

29. A. M. Gupta, *Macromolecules,* **24,** 3459 (1991).

30. D. Shimp, S. J. Ising, and J. R. Christenson, in *SAMPE Symposium,* Reno, NV, 1989, Vol. 34, p. 222.

31. M. Bauer and R. Gnauck, *Acta Polym.,* **38,** 658 (1987).